



# Investigating the Performance of Geogrid Reinforced Unbound Layer Using Light Weight Deflectometer (LWD)

Mohammadreza Sabouri<sup>1</sup> · Sahand Khabiri<sup>2</sup> · Seyed Mohammad Asgharzadeh<sup>3</sup> · Seyed Farhad Abdollahi<sup>1</sup>

Received: 8 December 2019 / Revised: 11 January 2021 / Accepted: 24 January 2021 / Published online: 9 June 2021  
© The Author(s), under exclusive licence to Chinese Society of Pavement Engineering 2021

## Abstract

This study investigates the performance of geogrid-reinforced unbound pavement layer. In this study, geogrid was used in various layouts and numbers using three different gradation of granular materials. Light weight deflectometer (LWD) device is known as a useful tool to evaluate the stiffness of unbound pavement layers. In this study, the LWD was utilized to experimentally investigate factors affecting the performance of geogrid reinforcement, including the number of geogrids, geogrid layout, and the gradation of unbound layer. There are several parameters which affect the LWD test results including the hammer weight, the falling height, and the surface stress. The effect of these parameters was also investigated. The results indicated that the improving effect of geogrid reinforcement is highly dependent upon the gradation of unbound layer. Incorporation of geogrid on the well-graded unbound layer decreased the elastic modulus; while, improving effect of geogrid reinforcement was observed on coarse and gap-graded unbound layers. It was also shown that geogrid reinforcement shows the best performance when one geogrid layer is installed at the bottom half of the unbound layer. The results of the LWD test showed that the LWD measurement at a particular hammer weight and falling height could be calibrated to a standard setting using the hammer's gravitational energy concept.

**Keywords** Geogrid · Unbound layer · Light weight deflectometer (LWD) · Geogrid layout · Elastic modulus

## 1 Introduction

Pavement structure is designed to alleviate the traffic load stresses to a tolerable level for the subgrade layer. The increasing demand for heavier vehicles and higher traffic volumes have increased interest for construction of stronger pavements which could be achieved by incorporation of

stiffer base and/or subbase layers. Moreover, increasing the stiffness of fairly inexpensive base layer may work in the way of reducing the required thickness of more expensive surface layers, which eventually could result in lower construction cost and higher environmental benefits. Mechanical stabilization of the base and subbase layers and incorporation of reclaimed asphalt pavement (RAP) are some of the methods to increase pavement structure stiffness [1, 2]. Installation of reinforcement in the unbound layer is another way to increase the stiffness of these layers which has proven to be able to extend the service life of the pavement [3]. Geogrid is a type of geosynthetic materials with a set of connecting tensile ribs with apertures that surrounding aggregates could penetrate in [4]. Geogrid is usually placed over the subgrade or within the base layer to improve its load carrying capacity. Geotextile is also a type of geosynthetic materials with additional functions compared with geogrid such as separation, drainage, and filtration [5].

The base layer thickness will be reduced in the presence of the geogrid, which results in a lower consumption of material and energy [6, 7]. Some studies have shown that incorporation of geogrid into the base layer leads to a

✉ Mohammadreza Sabouri  
sabouri@sharif.edu

Sahand Khabiri  
tul15251@temple.edu

Seyed Mohammad Asgharzadeh  
sm.asgharzadeh@modares.ac.ir

Seyed Farhad Abdollahi  
farhad.abdollahi@student.sharif.edu

<sup>1</sup> Department of Civil Engineering, Sharif University of Technology, Tehran, Iran

<sup>2</sup> Department of Civil Engineering, Temple University, Philadelphia, PA, USA

<sup>3</sup> Department of Civil and Environmental Engineering, Tarbiat Modares University, Tehran, Iran

decrease in the permanent deformation related distresses and therefore, results in a better serviceability of the roadway [8–10]. It has also been reported that the installation of the geogrid could reduce the vertical pressure at the bottom of the base layer by 28–39% [11].

Many researchers have studied the effect of shape and opening of geogrid on providing the interlock between aggregate and geogrid mesh and eventually, lateral constraint. These studies have shown that using geogrid in unbound layers increases the layers' elastic modulus [12–15]. The increase in the elastic modulus is mainly due to the increase in interaction between the aggregates and the geogrid mesh, which depends on the shape and size of the geogrid apertures, type and gradation of aggregate, and size and tensile strength of the geogrid bars [16, 17]. Other important parameters which affect the effectiveness of reinforced unbound layer are the number of geogrid layers and their locations. It has been shown that using two geogrids at the bottom and upper one-third location of unbound layer thickness yields in the best performance [10]. However, if just one geogrid is used, upper one-third location of unbound layer thickness results in a slightly better performance compared to being located at the middle of the unbound layer [10, 18]. Also, the installation of the geogrid in the middle of the unbound base layer has been reported to reduce the average vertical strain of the base layer under the implemented traffic load by about 10% [19]. Even though several studies have resulted in an increased layer modulus due to geogrid addition, some studies have reported no measurable benefits from geogrids in improving elastic modulus or resilient response of the base layer [20, 21].

Falling weight deflectometer (FWD) device is designed to measure the deflection basin caused by a known load exerted to pavement surface and back-calculating the elastic moduli of different pavement layers. However, application of FWD may have some difficulties, such as fairly high cost and low mobility on unpaved roads. Light weight deflectometer (LWD) was introduced to overcome the aforementioned limitations of FWD for conducting tests on unbound layers. The LWD test is also fairly simple to run and requires less technician training compared to FWD.

Elastic modulus is commonly used to evaluate the stiffness of soil and unbound materials. This parameter was introduced as the leading parameter to classify the behavior of subgrade, subbase, and base layers in pavement design. Non-destructive tests such as LWD has gained attention to estimate the elastic modulus of unbound layers. In the recent years, LWD has been widely used for quality control and verification of the layers' compaction. Several variables affect the results of this test. Some studies have been carried out to evaluate the reliability and repeatability of the results; a number of studies were conducted to investigate the effects of different variables including temperature, bumpers, loading plate diameter, hammer weight,

and falling height, on the LWD results [22, 23]. Material parameters also affect the LWD results, including gradation, density, moisture content, and type of unbound material [24].

Despite the presence of several geophones in FWD device to measure the deflection basin, LWD uses only one geophone which measures the deflection at the center of the loading plate. Therefore, the measured elastic modulus from LWD is affected by the stiffness of all the layers below the loading point, so the influence depth of the device plays an important role in the reliability of the results. Several studies have been performed to investigate this parameter. In early studies, the influence depth of LWD device was reported to be the same as loading plate diameter [25]. Another study reported that the influence depth is in the range of 1.2–1.4 times the loading plate diameter [26]. Later, some other researchers have found it to be 0.5–1.8 times the loading plate diameter depending on the hammer weight [27, 28]. Modeling LWD using finite element method has also been investigated and the influence depth has been reported as 2.0–2.5 and 2.0–3.5 times the loading plate diameter based on the stress and strain criteria, respectively. The stress and strain criteria are defined as the depth at which 10% of the surface stress and surface strain remains, respectively [29].

## 2 Objectives and Scope

This study aims to evaluate the elastic modulus of unbound base layers with different gradations and geogrid reinforcement states (i.e., the number of geogrids and the geogrid layout). Also, the effect of different testing conditions is investigated through laboratory testing. For this purpose, a full-scale box was prepared, and both the subgrade and base layers were installed for different unreinforced and geogrid-reinforced conditions. This study investigates the effect of several parameters including the gradation of unbound layer, the number and layout of geogrids, and the parameters associated with LWD (the hammer weight, the falling height, and the surface stress) on the measured elastic modulus of unbound layer.

## 3 Test Method

The LWD test was conducted in accordance with ASTM E2583-07 [30]. According to the elastic layered theory, the elastic modulus can be calculated using Eq. (1) in the influence zone of the LWD device [31]:

$$E = \frac{S \times q \times r(1 - \mu^2)}{\delta}, \quad (1)$$

where  $E$  is the elastic modulus;  $S$  is the stress distribution factor (2 for flexible pavements and  $\pi/2$  for rigid pavements

[32];  $q$  is the uniform stress applied to the loading plate of LWD;  $r$  is the radius of loading plate;  $\mu$  is the Poisson's ratio (in the range of 0.3–0.45 for unbound layers); and  $\delta$  is the maximum measured deflection. The uniform stress applied to the loading plate can be calculated using Eq. (2):

$$q = \frac{P}{A}, \quad (2)$$

where  $A$  is loading plate area and  $P$  is the maximum impact force which is directly measured by the LWD device during testing.

To better correlate the effects of the hammer weight and falling height parameters with the LWD results, the hammer's gravitational energy concept is introduced. In LWD testing, the hammer is released from a known height and strikes with the loading plate. According to Physics, the kinetic energy of an impacting body is mainly converted to the strain energy in the target body and partially dissipated through friction. Moreover, the kinetic energy of the LWD hammer, as an impacting body, at the moment of impact is equal to its gravitational energy before release. The gravitational energy can be simply calculated using Eq. (3):

$$U = W \times H \times g, \quad (3)$$

where  $U$  is the gravitational energy of hammer before release;  $W$  is the hammer weight,  $H$  is the falling height, and  $g$  is the gravity acceleration. Therefore, the gravitational energy could represent the impact intensity and can be used to better evaluate the effect of hammer weight and falling height on the measured elastic modulus.

## 4 Materials

In this study, the unbound materials were provided from a siliceous river soil query.

Three different gradations were selected for unbound base layer to evaluate the effect of soil gradation on the measured elastic modulus. These three gradations were selected following the lower, the middle, and the upper limits of the fifth grade in accordance with AASHTO M 147 [33] to generate coarse, medium, and fine gradations. According to the Unified Soil Classification System (USCS), the coarse, medium, and fine gradations are classified as GP, GW, and SP-SM, respectively. These soils are all classified as A-1-a based on the AASHTO soil classification system [34]. Figure 1 shows the gradations used in this study. According to the standard procedure of AASHTO T 180 [35], the optimum moisture content of the fine, medium and coarse gradation was 6.5, 6.0, and 5.6%, respectively. The maximum dry densities were equal to 2170, 2170, and 2180 kg/m<sup>3</sup> for fine, medium, and coarse gradations, respectively.

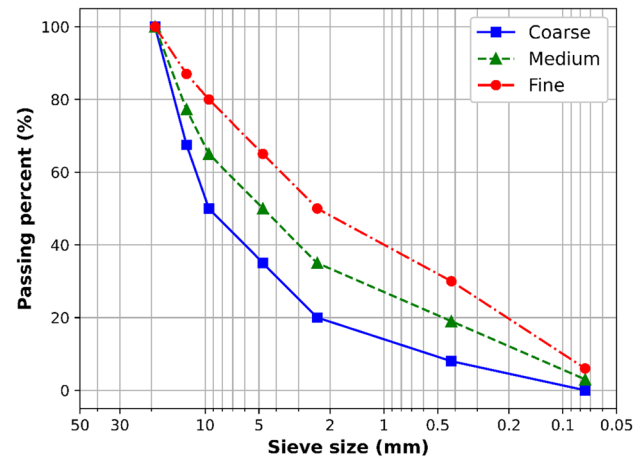


Fig. 1 Different gradations of unbound base layer

An unbound layer with a CBR of 10 was used as subgrade. According to the AASHTO classification system [34], the subgrade soil is classified as A-2-6 with a maximum dry density of 1940 kg/m<sup>3</sup> and an optimum moisture content of 12.6%.

To install subgrade and base layers in a controlled manner, the materials were first oven dried to remove the residual moisture content. The weight of each layer was then calculated based on the cross-section area of the experimental box, the layer height, and the density of the material at its optimum moisture content assuming 100% compaction. The amount of water required to bring each material to its optimum moisture content was then thoroughly mixed with the dry material using a bucket mixer. The material was then dumped into the experimental box and uniformly compacted using a vibratory compactor until a pre-determined layer height was obtained. The base layers were compacted in a minimum of three layers based on the geogrid(s) location. In each step, a portion of the base layer was installed and compacted. To ensure a uniform water content distribution within each layer, two soil samples were obtained from the top and bottom of each layer and tested for water content. All the test results were within  $\pm 0.3\%$  of the target optimum moisture content.

A third-generation polyester geogrid is used in base layer as reinforcement. The geogrid and its properties are shown in Fig. 2 and Table 1, respectively. No anchoring was used for geogrid installation.

## 5 Experimental Plan

All the LWD tests were performed in a full-scale cubical box with dimensions 1000 mm  $\times$  1000 mm  $\times$  1000 mm as shown in Fig. 3. These fairly large dimensions were selected



**Fig. 2** Geogrid used in this study

to avoid the effect of side confinement on the LWD results. A PRIMA 100 device was utilized in this study in which the maximum displacement of the tested unbound layer and the peak load are measured for calculating the layers' elastic modulus. The subgrade and base layers were both 150 mm in

thickness. A relatively thick base layer was selected to make sure it captures the entire influence zone of the LWD device.

As it was discussed before, in the current study, the LWD test was performed on the control (no geogrid) and reinforced base with one or two geogrid layers. A total of eight different reinforced conditions were evaluated as shown in Fig. 4 including the control (1 condition), a single geogrid at the bottom half, middle, and upper half of the base layer (3 conditions), two geogrids attached at the bottom half of the base layer (1 condition), two geogrids distanced by 35 mm at the bottom and upper halves of the base layer (2 conditions), and two geogrids distanced by 70 mm at the middle of the base layer (1 condition). The geogrid locations in the bottom and upper locations were 40 mm apart from either the bottom or the top of the base layer which is almost equal to one-third of the base layer's height. All the study parameters are listed in Table 2. It should be noted that a full factorial of the falling heights and hammer weights were not carried out; for the falling height of 500 mm, three different hammer weights were tested. The hammer weight of 15 kg was also tested at three different falling heights bringing the total different combinations of height and weight to five. As such, a total of 108 LWD tests were performed in this study. Each LWD test was repeated 3 times at the same location satisfying a maximum error of 3% among the replicates.

**Table 1** Geogrid properties

Properties	Test method	Geogrid 30*30
Layer material	–	Polyester
Unit weight ( $\text{g}/\text{m}^2$ )	EN ISO 9864	320
Maximum tensile strength (kN/m)	EN ISO 10319	$\geq 30$
Nominal strength strain (%)	EN ISO 10319	$\leq 8$
Tensile strength at 1% strain (kN/m)	EN ISO 10319	7.5/7.5 <sup>a</sup>
Tensile strength at 2% strain (kN/m)	EN ISO 10319	13.5/13.5 <sup>a</sup>
Tensile strength at 5% strain (kN/m)	EN ISO 10319	24/24 <sup>a</sup>
Geometric dimension of apertures (mm.mm)	–	34*34
Resistance against UV radiation (%)	EN 12224	96.3

<sup>a</sup>The first and second numbers refer to *x* and *y* directions, respectively

**Fig. 3** Testing box



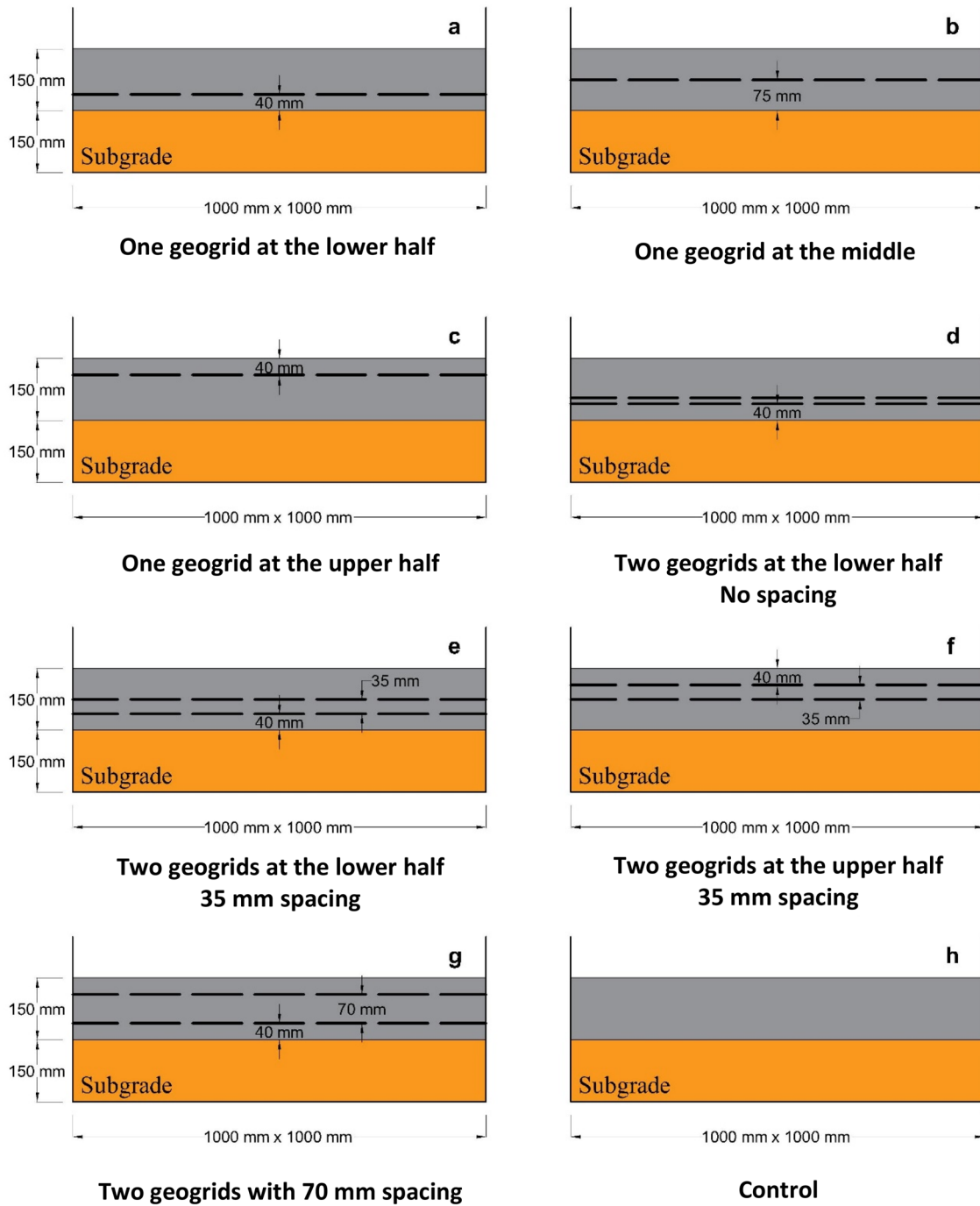


Fig. 4 Schematic of different geogrid layouts

Table 2 LWD test conditions

Condition	Base gradation	Loading plate diameter (mm)	Falling height (mm)	Hammer weight (kg)
Unreinforced/one layer of geogrid	Fine, medium, and coarse	100, 300	100, 300, and 500	5, 10, and 15
Two layers of geogrid				5 and 15

Also, all the testing points were placed at least 300 mm away from the walls of the testing box to minimize the potential boundary effects.

## 6 Results and Discussions

### 6.1 Effect of Gradation on the Elastic Modulus

Figure 5 shows the elastic modulus for different geogrid layouts and base layer gradations which was measured using 15 kg hammer falling from 500 mm height on the 100 mm diameter loading plate. As this figure suggests, geogrid installation increases the elastic modulus for both the fine and coarse gradations. In particular, application of a single geogrid at the lower location results in 43% and 35% increase in the elastic modulus for the coarse and fine base layer gradations, respectively. The higher increase in elastic modulus in the case of coarse gradation suggests that geogrid installation is an effective way to increase aggregate interlocks of the coarse graded unbound materials.

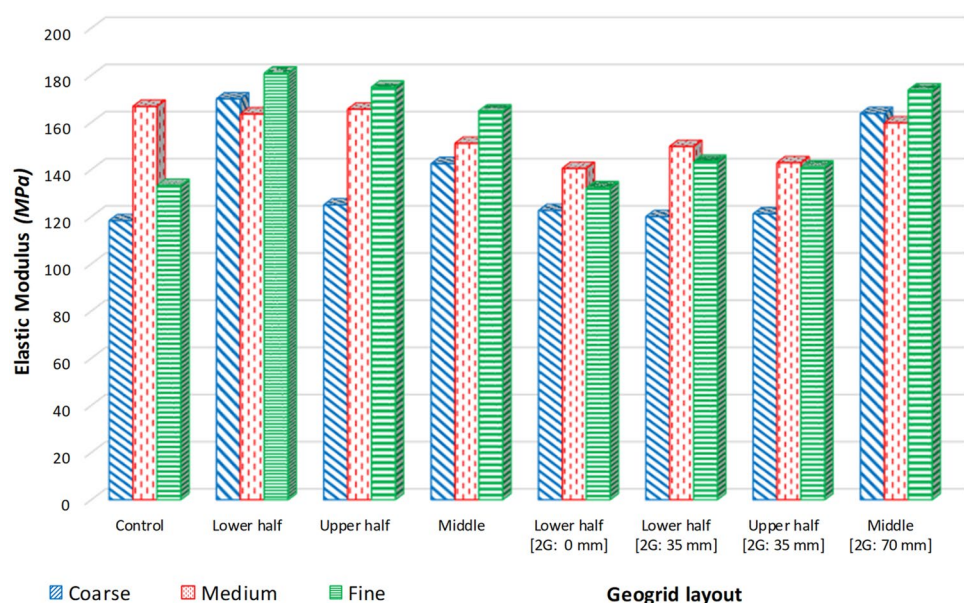
Figure 5 also suggests that when no geogrid is used, the medium gradation results in a higher elastic modulus compared to the other two gradations. This may be because the medium gradation was classified as an s-shaped well-graded gradation in accordance with USCS and therefore, it has stronger aggregate interlocks. It is also interesting to note that the application of geogrid reinforcement in the case of medium gradation decreases the elastic modulus as the geogrid may reduce the aggregate interlocks that were already existed in the material's structure. Application of the geogrid for the medium gradation in the best

case (single geogrid at the lower location) results in about the same elastic modulus as for the control case with no geogrids.

These results indicate that the effectiveness of geogrid reinforcement is highly dependent upon the gradation of the unbound layer. In another word, the geogrid properties should be carefully selected regarding the gradation of the unbound layer.

Despite the medium gradation, both of the fine and coarse gradations get benefited from the installation of the reinforcement. In other words, the application of geogrid seems to be specifically beneficial for poorly graded and gap-graded materials. In another study carried out by Vangla and Gali, the best performance of geogrid reinforcement was obtained when there was a proper balance between the geogrid apertures and the aggregate size [36]. They introduced the asperity ratio defined as the ratio of the geogrid asperity size, which is equal to the space between two consecutive strands of the geogrid divided by the mean particle size of the unbound material, and concluded that the best performance can be achieved when the asperity ratio is close to one [36]. However, the asperity ratios for coarse, medium, and fine gradations of the current study are 3.1, 6.3, and 12.7, respectively, which are significantly higher than the suggested asperity ratio of one. This might be due to the significant different geogrid mesh size that has been utilized in the current study compared with Vangla and Gali's study. Another study has reported that the elastic modulus decreases with an increase in the fine content when the fine content is significantly high and in the range of 20–80% [24].

**Fig. 5** Effect of gradation and geogrid layout on the elastic modulus (“2G” stands for two geogrids and their spacing is provided in brackets)



## 6.2 Effect of the Number of Geogrids and Their Layout on the Elastic Modulus

As it was mentioned before, implementation of the geogrid reinforcement for the medium gradation decreases the elastic modulus. On the contrary, the application of the geogrid improves the stiffness of base layer when the material is fine or coarse. As Fig. 5 shows, the worst performance happens when two geogrids are placed with no spacing (as illustrated in Fig. 4d). This may suggest that application of two geogrids with no spacing creates a weak point in the base layer and diminishes geogrid's effect of engaging and interlocking aggregates. However, incorporation of geogrids with 35 or 70 mm spacing improves the elastic modulus of the base layer. In particular, in the case of coarse gradation, an increase of 1.5%, 2.5%, and 38% in measured elastic modulus was observed when geogrids were spaced and located as presented in Fig. 4e–g, respectively which suggests a significant improvement in the elastic modulus of base layer when the spacing increases to 70 mm. As such, it can be concluded that providing a minimum distance between the geogrids may allow the unbound material to form aggregate interlocks in a more effective manner. It is also interesting to note that incorporation of geogrids with 35 mm of spacing seems to have a higher improving effect on the elastic modulus of the fine gradation (7.5% increase) compared with the coarse gradation (1.5% increase). Other studies have also reported that using two geogrids results in an increase in the stiffness of unbound layer [10, 18].

As Fig. 5 suggests, incorporation of a single geogrid in almost any locations within the unbound layer leads to an increase in the elastic modulus for both the fine and coarse gradations. This suggests that it is possible to compensate the negative effect of poorly graded and gap-graded gradation of unbound materials on their elastic modulus by incorporation of a geogrid reinforcement. Delving into the details, in the case of coarse gradation, installation of geogrid at the upper, middle, and lower locations of the base layer results in 5.5%, 20%, and 44% increase in elastic modulus, respectively. For the fine gradation, placing the geogrid at the middle of the base layer leads to the lowest improvement; but, the lower location still results in the highest improvement in elastic modulus. Therefore, it can be concluded that the best performance of geogrid installation can be obtained when the geogrid is placed at the lower location of the base layer as illustrated in Fig. 4a. This is while other researchers have reported that the application of a single geogrid reinforcement at the upper third and middle locations results in the largest increase in the elastic modulus [10, 18, 36]. This difference might be due to difference in the thickness of the base layers. Abu-Farsakh et al. have used a 305 mm unbound base layer which is almost two times of the thickness used in this study. In another study, installation of geogrid at the

depth of approximately half of the radius of the loading area has been reported as the optimum depth of geogrid installation, regardless of the base layers' thickness [7] which is not supported by the current study results; the half of the loading plate radius is 25 mm which is fairly similar to the case of upper half location of the geogrid in the current study. As the results show, the upper half location does not conclude in the best performance of geogrid.

Conclusively, it seems that the results of the measured elastic modulus could be classified into the three groups with respect to the different geogrid layouts. In this regard, application of a single geogrid at lower location and double geogrids with 70 mm spacing has shown the best performance followed by single geogrid at upper and middle locations of base layer, and then the remaining layouts using double geogrids. Also, except for the double geogrids with 70 mm spacing, the application of two geogrids not only increases the construction costs, but also deteriorates the performance of the base layer.

## 6.3 Effect of LWD Parameters on the Elastic Modulus

Figure 6 presents the LWD test results for different hammer weights, geogrid layouts, and gradation of base layer with the constant falling height of 500 mm. As Fig. 6 suggests, in general, increasing the hammer weight leads to an increase in the elastic modulus. Similarly, Fig. 7 shows the effect of the falling height on the elastic modulus for different geogrid layouts and gradation of the base layer when a 15 kg hammer is used. As this figure shows, the elastic modulus increases as the falling height increases in almost all the cases. These behaviors were expected due to the stress-dependent nature of the unbound granular materials. This also suggests that geogrid reinforcement does not affect this behavior.

According to Eq. (3), the hammer weight and falling height are directly related using the concept of gravitational energy ( $U$ ). As such, an increase in either the falling height or the hammer weight results in an increase in the gravitational energy. To assess the effect of the gravitational energy on the elastic modulus, the elastic modulus is plotted against the gravitational energy for different combinations of base layers' gradation, and geogrid layout as shown in Fig. 8. In this figure, five different values of gravitational energy are calculated using the different combination of hammer weights (5, 10, and 15 kg) and falling heights (100 mm, 300 mm, and 500 mm). A linear regression line is then fitted to each set of points. As expected, the elastic modulus generally increases with the increase in the gravitational energy. However, the rate of increase of the elastic modulus as a function of hammer's gravitational energy seems to be almost the same in each gradation. Table 3 shows these rates of increase and their basic statistical parameters (average

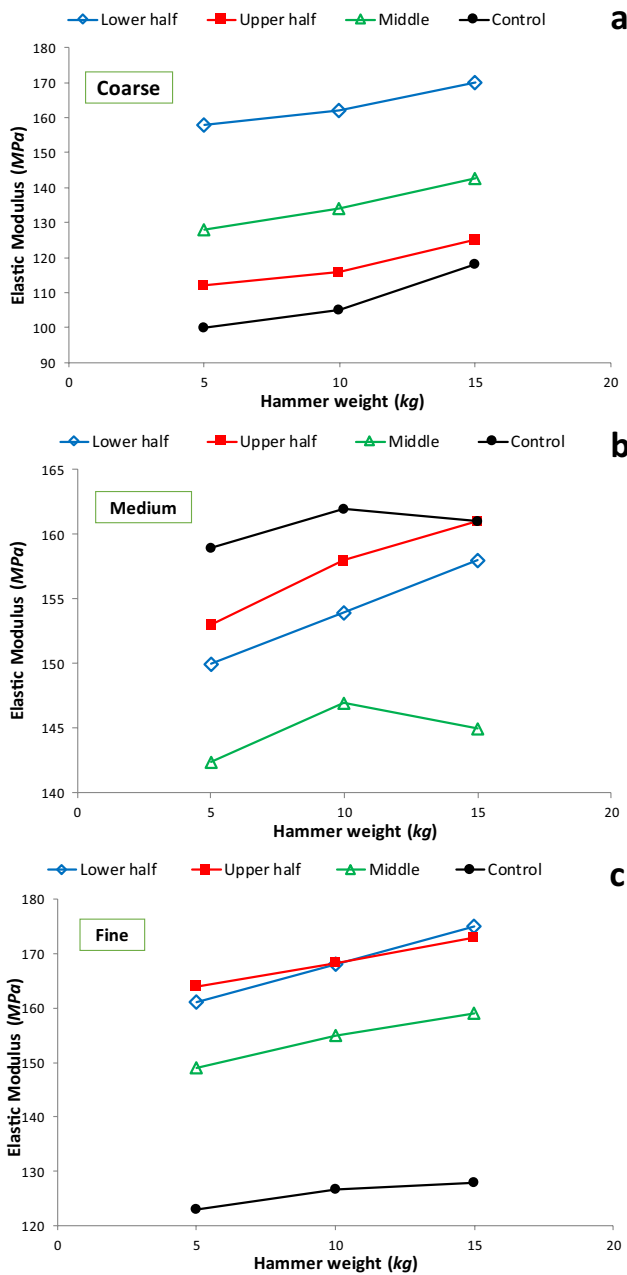


Fig. 6 Effect of the hammer weight on the elastic modulus

and standard deviation) to better interpret the results. As this table suggests, the average rate of increase for coarse and fine base layers are almost the same. It is worth mentioning that these results are obtained using the linear regression on the range of hammer’s gravitational energy from 5 to 75 J. Thus, the regression models are valid in this range. Table 3 also presents different rates of increase for different geogrid layouts along with their standard deviations.

It should be noted that in general, the results of the regression lines in Table 3 could be used as a correction factor to calibrate the measurements of elastic modulus with a

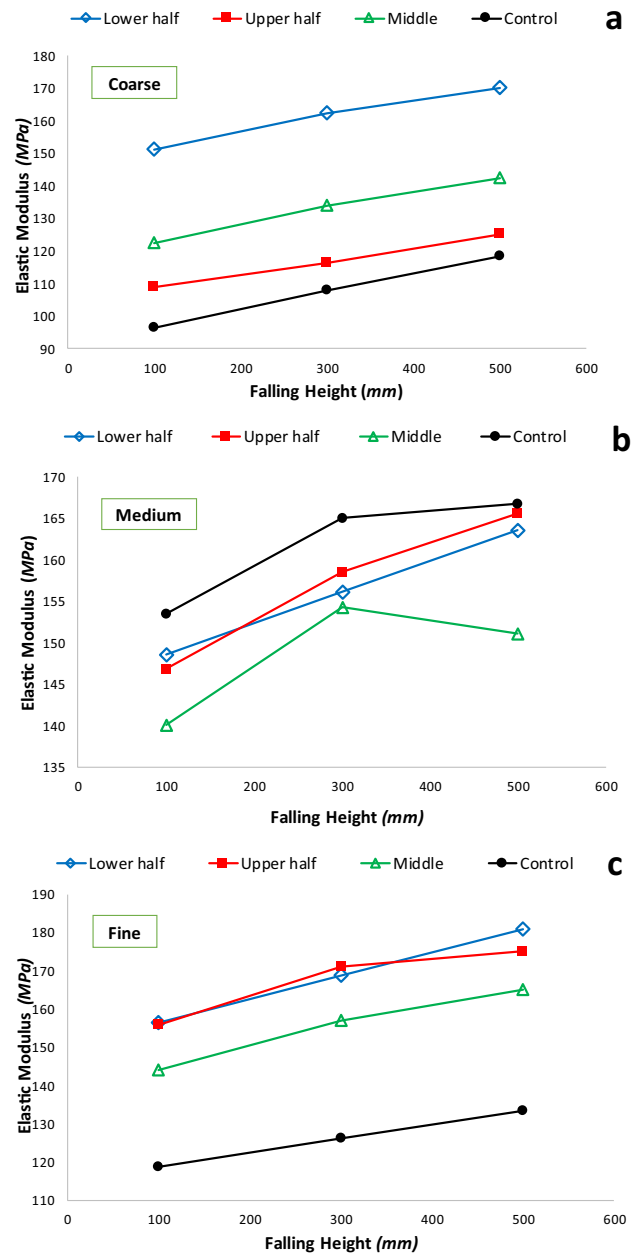


Fig. 7 Effect of the falling height on the elastic modulus

particular hammer weight and falling height setting to the one with standard setting. The only consideration in using Table 3 data is keeping the hammer’s gravitational energy in the range of 5–75 J.

### 7 Summary and Conclusions

In this study, the effect of different factors affecting the performance of geogrid reinforcement of unbound base layer were studied using the LWD device. These factors include



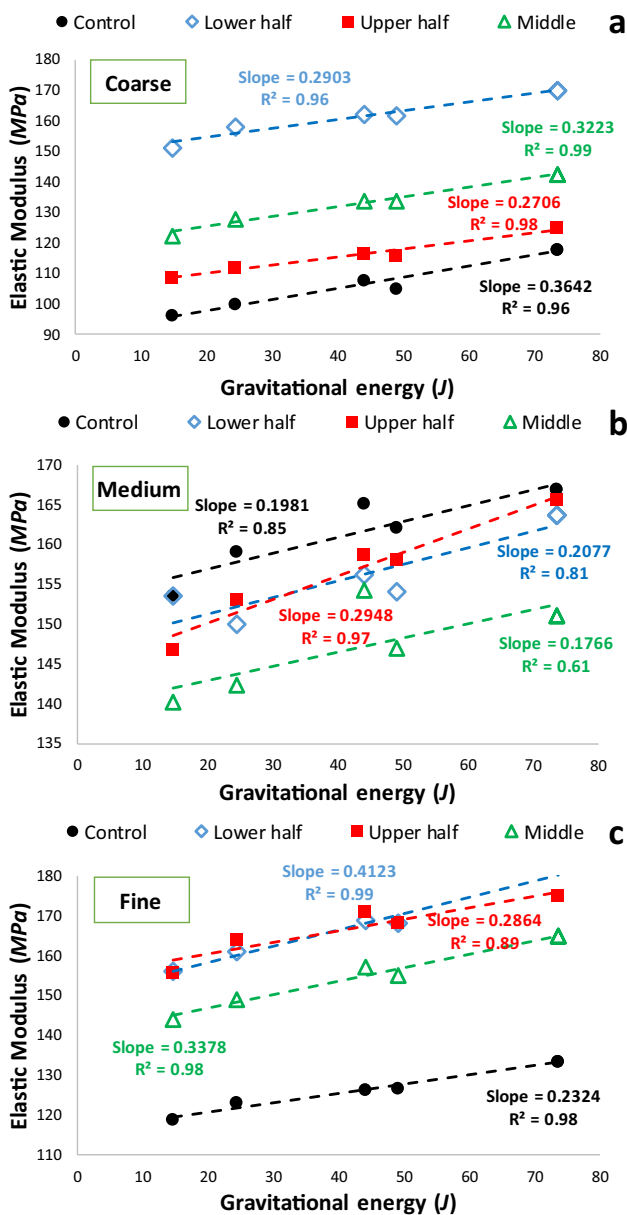


Fig. 8 Effect of the hammer’s gravitational energy on the elastic modulus for different cases

number of geogrids, geogrid layouts, and gradation of the base layer. In addition, the effect of LWD parameters on the results were studied. Based on the results of 108 LWD tests conducted in this study, the following conclusions can be drawn:

- Application of the geogrid reinforcement on fine and coarse gradations increases the elastic modulus. The opposite trend was seen for the medium gradation. It was concluded that the effectiveness of geogrid application is highly dependent on the gradation of the unbound layer. In other words, it is possible to improve the elastic modulus of coarse and gap-graded unbound materials to the equivalent of well-graded one using the geogrid reinforcement.
- Incorporation of the geogrid reinforcement in the case of medium gradation reduces the elastic modulus perhaps due to disturbing the aggregate interlocks that already exist in the stone matrix. Nevertheless, base layer with medium gradation has the highest elastic modulus among all different cases when no geogrid is installed.
- When a single geogrid is used, installation of the geogrid at the bottom half of the layer results in the best performance. When two geogrids are employed, the elastic modulus increases along with the increase of geogrid spacing from 0 to 70 mm.
- Increasing the hammer weight and/or falling height increases the hammer’s gravitational energy by which the elastic modulus increases. It was shown that the elastic modulus increases linearly with the increase in hammer’s gravitational energy. Thus, any measurement of elastic modulus with a particular LWD setting can be calibrated to the intended (standard) setting using the rate of increases shown in Table 3.

Table 3 Regression results of elastic modulus against hammer’s gravitational energy

Geogrid layout	Coarse gradation		Medium gradation		Fine gradation	
	Rate of increase	R <sup>2</sup>	Rate of increase	R <sup>2</sup>	Rate of increase	R <sup>2</sup>
Control	0.3642	0.96	0.1981	0.85	0.2324	0.98
Bottom half	0.2903	0.97	0.2077	0.81	0.4123	0.99
Upper half	0.2706	0.98	0.2948	0.97	0.2864	0.89
Middle	0.3223	0.99	0.1766	0.61	0.3378	0.98
Average	0.3119	–	0.2193	–	0.3172	–
Standard deviation	0.0354	–	0.0450	–	0.0663	–

## References

- Oliver, T., Wayne, M., & Kwon, J. (2018). Mechanical stabilization of unbound layers to increase pavement performance and incorporation of benefits into ME analysis. *Procedia Engineering*. <https://doi.org/10.1016/j.proeng.2016.06.153>
- Sabouri, M. (2014). Development of a unified fatigue failure criterion for asphalt mixtures and its applications to reclaimed asphalt pavement (RAP) mixtures, Doctoral dissertation, North Carolina State University
- Abu-Farsakh, M. Y., & Chen, Q. (2011). Evaluation of geogrid base reinforcement in flexible pavement using cyclic plate load testing. *International Journal of Pavement Engineering*. <https://doi.org/10.1080/10298436.2010.549565>
- Aran, S. (2006). Base reinforcement with biaxial geogrid: Long-term performance. *Transportation Research Record*, 1975, 115–123
- Guido, V. A., Chang, D. K., & Sweeney, M. A. (1986). Comparison of geogrid and geotextile reinforced earth slabs. *Canadian Geotechnical Journal*. <https://doi.org/10.1139/t86-073>
- Chen, Q., Abu-Farsakh, M. Y. (2012). Structural contribution of geogrid reinforcement in pavement. In *GeoCongress* (pp. 1468–1475)
- Mousavi, S. H., Gabr, M. A., & Borden, R. H. (2017). Optimum location of geogrid reinforcement in unpaved road. *Canadian Geotechnical Journal*. <https://doi.org/10.1139/cgj-2016-0562>
- Moghaddas-Nejad, F., & Small, J. C. (1996). Effect of geogrid reinforcement in model track tests on pavements. *Journal of Transportation Engineering*. [https://doi.org/10.1061/\(ASCE\)0733-947X\(1996\)122:6\(468\)](https://doi.org/10.1061/(ASCE)0733-947X(1996)122:6(468))
- Al-Qadi, I. L., Brandon, T. L., Bhutta, S. A. (1997). Geosynthetic stabilized flexible pavement. In *Conference on Geosynthetics* (pp. 619–632)
- Abu-Farsakh, M. Y., Akond, I., & Chen, Q. (2016). Evaluating the performance of geosynthetic-reinforced unpaved roads using plate load tests. *International Journal of Pavement Engineering*. <https://doi.org/10.1080/10298436.2015.1031131>
- Williams, S., Wright, J., Hanumasagar, S. S., Kim, S. S., & Frost, J. D. (2018). Large-scale and bench-scale test systems for assessing impact of geogrids on pavement founded on problematic soils. *Journal of Testing and Evaluation*. <https://doi.org/10.1520/JTE20180002>
- Perkins, S. W. (1999). Geosynthetic reinforcement of flexible pavements: Laboratory based pavement test sections. Report Number FHWA/MT-99-001/8138. Montana State University-Bozeman, Bozeman
- Al-Qadi, I. L., Dessouky, S., Kwon, J., & Tutumluer, E. (2008). Geogrid in flexible pavements: Validated mechanism. *Transportation Research Record*, 2045, 102–109
- Qian, Y., Han, J., Pokharell, S. K., & Parsons, R. L. (2013). Performance of triangular aperture geogrid-reinforced base courses over weak subgrade under cyclic loading. *Journal of Materials in Civil Engineering*. [https://doi.org/10.1061/\(ASCE\)MT.1943-5533.0000577](https://doi.org/10.1061/(ASCE)MT.1943-5533.0000577)
- Rajagopal, K., Chandramouli, S., Parayil, A., & Iniyan, K. (2014). Studies on geosynthetic-reinforced road pavement structures. *International Journal of Geotechnical Engineering*. <https://doi.org/10.1179/1939787914Y.0000000042>
- Tutumluer, E., & Kwon, J. (2006). Evaluation of geosynthetic use for pavement subgrade restraint and working platform construction. *Geotechnical Applications for Transportation Infrastructure*. [https://doi.org/10.1061/40821\(181\)8](https://doi.org/10.1061/40821(181)8)
- Hatami, K., Mahmood, T., Zaman, M., Ghabchi, R. (2012). Development of ODOT guidelines for the use of geogrids in aggregate bases. Report Number OTCREOS9. 1-23F, Midwest: The University of Oklahoma
- Abu-Farsakh, M. Y., Souci, G., Voyiadjis, G. Z., & Chen, Q. (2012). Evaluation of factors affecting the performance of geogrid-reinforced granular base material using repeated load triaxial tests. *Journal of Materials in Civil Engineering*. [https://doi.org/10.1061/\(ASCE\)MT.1943-5533.0000349](https://doi.org/10.1061/(ASCE)MT.1943-5533.0000349)
- Gu, F., Luo, X., Zhang, Y., Chen, Y., Luo, R., & Lytton, R. L. (2018). Prediction of geogrid-reinforced flexible pavement performance using artificial neural network approach. *Road Materials and Pavement Design*. <https://doi.org/10.1080/14680629.2017.1302357>
- Tang, X., Stoffels, S. M., & Palomino, A. M. (2013). Resilient and permanent deformation characteristics of unbound pavement layers modified by geogrids. *Transportation Research Record*, 2369, 3–10. <https://doi.org/10.3141/2369-01>
- Tingle, J. S., & Jersey, S. R. (2009). Full-scale evaluation of geosynthetic-reinforced aggregate roads. *Transportation Research Record*, 2116, 96–107. <https://doi.org/10.3141/2116-13>
- Fleming, P. R., Frost, M. W., Lambert, J. P. (2009). Light Weight Deflectometer for quality assurance in road construction. In *8th International Conference Bearing Capacity Road Railways and Airfields* (pp. 809–818)
- Posribink, T., Konglitkul, W., Youwai, S., Jongpradist, P., Punthutacha, K. (2012). Influence of falling height and plate size on surface stiffness evaluated by LWD. In *International Conference on High Voltage Engineering* (pp. 361–368)
- George, V., & Kumar, A. (2017). Effect of soil parameters on modulus of resilience based on portable falling weight deflectometer tests on lateritic subgrade soils. *International Journal of Geotechnical Engineering*. <https://doi.org/10.1080/19386362.2017.1403075>
- Fleming, P. R., Frost, M. W., Rogers, C. D. F. (2000). A comparison of devices for measuring stiffness in situ. In *International Symposium Unbound Aggregates Road*, UNBAR 5 (pp. 193–200)
- Nazzal, M., Abu-Farsakh, M. Y., Alshibli, K., Mohammad, L. (2004). Evaluation the potential use of a portable LWD for characterizing pavement layers and subgrades. In *Geotechnical Engineering for Transportation Projects* (pp. 915–924)
- Mooney, M. A., & Miller, P. K. (2009). Analysis of light weight deflectometer test based on in situ stress and strain response. *Journal of Geotechnical and Geoenvironmental Engineering*. [https://doi.org/10.1061/\(ASCE\)1090-0241\(2009\)135:2\(199\)](https://doi.org/10.1061/(ASCE)1090-0241(2009)135:2(199))
- Senseney, C., & Mooney, M. (2010). Characterization of two-layer soil system using a light weight deflectometer with radial sensors. *Transportation Research Record*, 2186, 21–28
- Tirado, C., Mazari, M., Carrasco, C., & Nazarian, S. (2015). Evaluating influence depth of light weight deflectometer through finite element modeling. *Airfield and Highway Pavements*. <https://doi.org/10.1061/9780784479216.070>
- ASTM E2583. (2015). Standard test method for measuring deflections with a light weight deflectometer (LWD). American Society for Testing and Materials
- Nassar, W., Al-Qadi, I. L., Flintsch, G. W., Appea, A. (2000). Evaluation of pavement layer response at the Virginian smart roads. In: *Pavement Subgrade, Unbound Materials, and Nondestructive Testing* (pp. 104–118)
- George, K. P. (2006). Portable FWD (PRIMA 100) for in-situ subgrade evaluation. Report Number FHWA/MS-DOT-RD-06-179. University of Mississippi, Mississippi
- AASHTO M 147. (2008). Standard specification for materials for aggregate and soil-aggregate subbase, base, and surface courses. American Association of State Highway and Transportation Office
- AASHTO M 145. (2012). Standard specification for classification of soils and soil-aggregate mixtures for highway construction purposes. American Association of State Highway and Transportation Office
- AASHTO T 180. (2012). Standard method of test for moisture-density relations of soils using a 4.54-kg rammer and a 457-mm drop. American Association of State Highway and Transportation Office
- Vangla, P., & Gali, M. L. (2016). Effect of particle size of sand and surface asperities of reinforcement on their interface shear

behavior. *Geotextiles and Geomembranes*. <https://doi.org/10.1016/j.geotexmem.2015.11.002>



**Mohammadreza Sabouri, PhD, PE** earned his doctoral degree on asphalt pavement materials from North Carolina State University. He is currently an Assistant Professor at Sharif University of Technology. His research interests are generally focused on characterizing and performance modelling of pavement materials, pavement systems, and pavement design, analysis and development. He has many publications and invited presentations at different international journals and conferences.



**Sahand Khabiri** received his MSc degree in Transportation and Highway Engineering from Tarbiat Modares University. He is currently a PhD candidate at Temple University, Philadelphia, USA. His research interests include lightweight and sustainable materials, non-destructive testing (NDT), geosynthetics, artificial neural network, and machine learning.



He has many publications and presented presentations at different international journals and conferences.

**Seyed Mohammad Asgharzadeh, PhD** earned his doctoral degree in Transportation Engineering from Sharif University of Technology. He has served as an assistant professor at Tarbiat Modares University from 2014 to 2018 while his research activities were mainly focused on the performance properties of asphalt binders and mixtures. He is currently working as a research scientist at University of British Columbia, Vancouver. He has many publications and presented presentations at different international journals and conferences.



**Seyed Farhad Abdollahi** received his MSc degree in Pavement Engineering from Sharif University of Technology where he worked on bituminous materials testing, modeling, non-destructive testing, and soil improvement. He is currently a research assistant at the Michigan State University. His current research is focused on nonlinear pavement analysis and design using finite element and layered elastic methods.